Characteristics of Laser Diodes Influenced by Electron-Dominant Nonuniform Carrier Distribution

Bing-Ruey Wu[a], Ching-Fuh Lin[a], Lih-Wen Laih[b] and Tien-Tsorng Shih[b]

[a] Department of Electrical Engineering and Graduate Institute of Electro-Optical Engineering

National Taiwan University, Taipei 106, Taiwan

[b] Telecommunication Laboratory, Chunghua Telecom Co., Ltd., Yang-Mei, Taiwan

ABSTRACT

Electron-determined nonuniform carrier distribution inside multiple quantum wells (MQW) is experimentally discovered. Two groups of mirror-imaged nonidentical quantum well (QW) InGaAsP/InP lasers diodes are designed, fabricated, and measured. Measured characteristics of both groups show that electron, instead of hole, is the dominant carrier affecting carrier distribution. Carrier transport effects including carrier diffusion/drift and capture/emission processes inside MQW are described to explain the nonuniform carrier distribution. The reason for the electron dominated carrier distribution is because electron takes less time to be captured into QW two-dimensional (2D) states than hole does. The sequence of the nonidentical QWs is also shown to have significant influence on device characteristics.

1. INTRODUCTION

Quantum well (QW) engineering is a convenient way to manipulate the bandgap energy of compound semiconductor materials. Multiple-quantum-well (MQW) semiconductor lasers have the advantages of higher differential gain, wider modulation bandwidth, and better temperature characteristics than bulk-material semiconductor lasers. [1] These advantages make MQW lasers attractive to all fields of applications, including optical communication. However, the dynamic properties of quantum well semiconductor lasers are not better than bulk material lasers until the 90's [2] when the carrier dynamics are taken into account for the QW design. Due to the quantization nature of QWs along the epitaxial axis, complicated carrier dynamics are involved therein.[3] Contemporary models describing carrier dynamics involve carrier diffusion/drift across the unquantized 3D structure, and the processes by which carriers are captured into and escape from the QWs. These processes cause the transport delays, and degrade the dynamic properties of MQW lasers. Thus designing such MQW structures for improved performance is not straightforward. Carrier dynamics need to be understood in advance.

*Correspondence: Email: cflin@cc.ee.ntu.edu.tw; Tel: 886-2-23635251 ext. 339; Fax: 886-2-23638247

Physics and Simulation of Optoelectronic Devices IX, Yasuhiko Arakawa, Peter Blood, Marek Osinski, Editors, Proceedings of SPIE Vol. 4283 (2001) © 2001 SPIE · 0277-786X/01/$15.00

Calculations using rate equation approaches[4] have shown that the carrier inside the MQW structures are not uniform, and had been verified experimentally.[5, 6]

When MQW lasers are forward biased, electrons inject from n-cladding layer and holes injected from the opposite direction, causing a nonuniform carrier distribution. Studies have defined the "dominant carrier" as the carrier from which side the carrier distribution density is higher because it determines the carrier distribution. Past researches suggest the dominant carrier is hole (means carrier distribution density near p-cladding layer is higher) because, first, the larger density of state in the valence band than conduction band. Carrier capture rate is proportional to the density of states (DOS), so hole has shorter capture time into QW states than electron. The shorter capture time enables hole to be captured into QWs faster than electron. In addition, electrons have higher mobility and longer capture time than holes, so electrons distribute according to the hole distribution in order to achieve quasi charge neutrality.[3, 7]

This work shows evidence of an opposite action. Electron-dominated behavior by utilizing nonidentical MQW lasers is observed experimentally. Nonidentical MQW lasers provide a direct way to study the carrier distribution of MQW. [7] Two groups of mirror-imaged MQWs are designed. One consists of a pair of samples with four nonidentical QWs with four different well widths, and the other one consists of two types of QWs that correspond to 1.3μm and 1.55μm QWs, respectively. The designed samples are used to fabricate laser diodes. Optical characteristics are measured. The results show that the dominant carrier is electron. The reason is attributed to the long separate confinement heterostructure (SCH) region length.

2. EXPERIMENT

Two different groups of mirror-imaged nonidentical MQWs are designed to exploit the carrier distribution properties inside MQW structures. They will be described respectively.

2.1 Mirror-Imaged Nonidentical MQW Group I

2.1.1 Nonidentical MQW Design and Fabrication

Layer structure of group I is shown in Fig. 1. Both consist of four quantum wells of four different widths – 15nm, 6nm, 4nm, and 2.2nm. The well material is $In_{0.56}Ga_{0.44}As_{0.95}P_{0.05}$ and the wells are bounded by 15nm $In_{0.79}Ga_{0.21}As_{0.45}P_{0.55}$ barrier. The separate confinement heterostructure (SCH) region for both 05111 and 05112 is 120nm $In_{0.79}Ga_{0.21}As_{0.45}P_{0.55}$. 05112 and 05111 have the 15nm well nearest to the n-cladding and p-cladding layers, respectively, while other wells are placed in the order according to their widths. The calculated emission wavelengths of the four QWs are 1.51μm, 1.43μm, 1.37μm, 1.3μm, respectively.

The nonidentical MQW structures are grown on InP substrate with lattice-matched condition by MOCVD. The grown nonidentical MQW structures are then used to fabricate ridge-waveguide laser diodes (LDs) by standard processing procedures. The ridge waveguide was created by electron cyclotron resonance-reactive ion etch (ECR- RIE). The etching

was stopped at ~100nm above the SCH layer. The devices are about 500μm long.

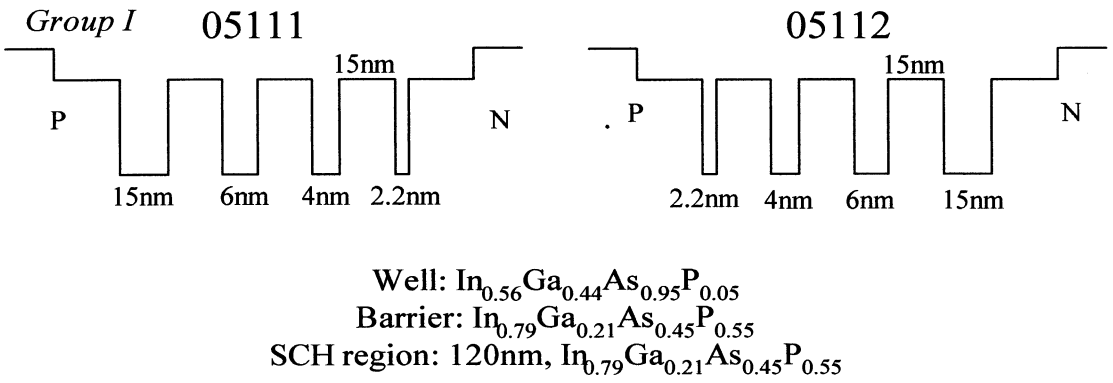

Fig. 1 Layer structure of group I mirror-image nonidentical MQW, 05111 and 05112

2.1.2 Device Characteristics

Optical characteristics such as lasing spectra and light-output power relations under temperature varying from 20℃ to 55℃ are measured on fabricated devices. The spectra of the fabricated lasers in room temperature are measured and shown in Fig. 2. The 05111 LD has the lasing wavelength at 1501.36nm and the 05112 LD has the lasing wavelength at 1483.68nm. Both lasing wavelengths correspond to the emission of widest 15nm quantum well. Threshold current (I_{th}) and differential quantum efficiency (η_d) versus temperature diagrams are shown in Fig. 3. I_{th} of 05111 LDs is 91.15mA and 106.5mA at 20°C and 25°C, respectively, while I_{th} of 05112 LDs is 46.38mA and 57.21mA at 20°C and 25°C, respectively. The experiments show that 05112 LDs have the I_{th} only half of 05111 LDs, as shown in Fig. 3(a), although both types of LDs have their lasing wavelength contributed from the 15nm QW. Characteristic temperature of 05111 and 05112 are 39.13K

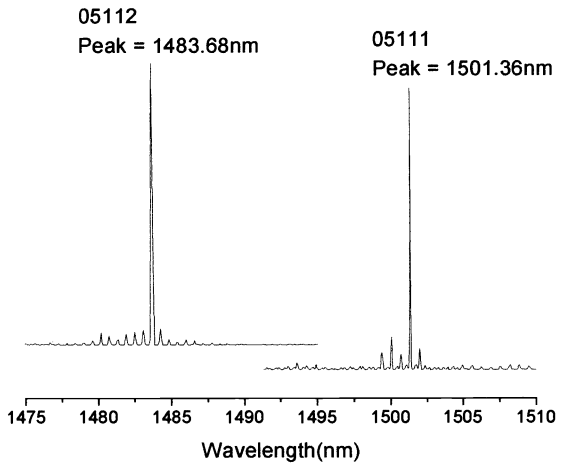

Fig. 2 Measured lasing spectra of 05111 and 05112. Both lasing wavelengths correspond to the 15nm QW.

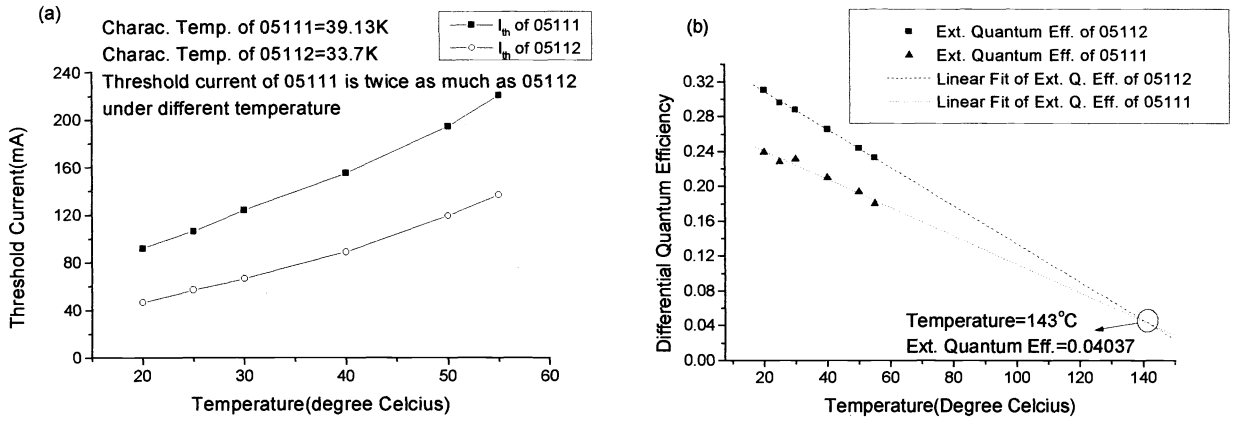

Fig. 3 (a) Threshold current and (b) differential quantum efficiency of 05111 and 05112 measured in different temperature.

And 33.7K, respectively, showing that 05112 LDs are more sensitive to temperature than 05111 LDs. Differential quantum efficiency η_d vs. temperature is shown in Fig. 3(b). η_d of 05111 LDs is 0.239 at 20°C while η_d of 05112 LDs is 0.311 at 20°C. Differential quantum efficiency of 05112 is higher than that of 05111 at all temperatures, although efficiencies degrade with rising temperature in both samples. Linear fit shows that external quantum efficiency of 05111 and 05112 will be the same at 143°C, which implies that, for T>143°C, carrier escape plays a much more important role on the carrier distribution than other factors like the well sequence. The larger negative slope of 05112 also indicates that 05112 LDs are more sensitive to temperature than 05111 LDs. This is consistent with the conclusion derived before.

Theoretical calculation using Luttinger-Kohn model[8] shows that among the four QWs, the wider QW has the higher gain under the same carrier density. In other words, because the loss is not sensitive to wavelength, the wider well can achieve lasing condition more easily. The threshold current of a laser diode is determined by its material gain, confinement factor, internal loss and mirror loss. Because the two samples have the same separate confinement heterostructure and waveguide structure, their internal loss, mirror loss, and confinement factor are approximately the same. This indicates that the difference in threshold (and lasing efficiency) comes from the different material gain at the same injection condition. From the above, the wider QW can achieve higher gain at a given carrier density. Also, measured results show that the threshold current of 05112 LDs is lower than that of 05111 LDs and lasing efficiency of 05112 is better than that of 05111. Referring to the layer structure of 05111 and 05112 in Fig. 1, 05112 has the 15nm QW near the n-cladding layer while 05111 has the 15nm QW close to the p-cladding layer. The fact that lasing wavelengths of 05111 and 05112 all correspond to the 15nm QW emission reveals that carrier distribution is larger in the QW near the n-cladding side. That is, electron is the dominant carrier in these nonidentical MQW structures. The conclusion that the carrier distribution inside the nonidentical MQWs of 05111 and 05112 is dominated by electron leads to the schematic illustration of carrier distribution shown in Fig. 4. Carrier distribution density is higher in the QW near the n-cladding layer. Combining the theoretical gain calculation and the

schematic figure, the experimental properties of 05111 and 05112 LDs can be explained. First, the 15nm QW can achieve lasing condition most easily, so the lasing wavelengths of both LDs correspond to the 15nm QW, namely 1.5μm. Second, due to the higher carrier density in 15nm QW for 05112, 05112 can achieve lasing condition easier than 05111, namely lower threshold current I_{th}. Third, because 05111 LDs also oscillate at the wavelength corresponding to 15nm QW, the less carriers captured in 15nm QW causes lower differential quantum efficiency of 05111 than 05112.

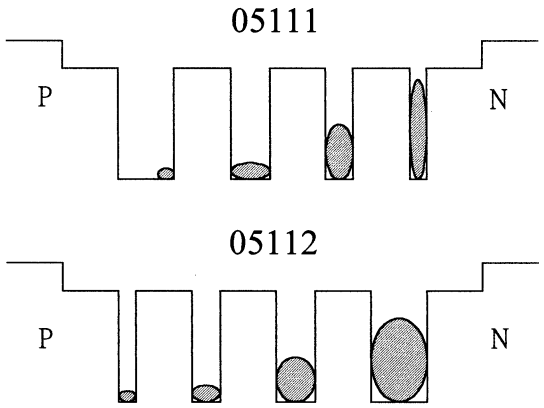

Fig. 4 Illustrated carrier distribution of 05111 and 05112 nonidentical MQW structures

2.2 Mirror-Image Nonidentical MQW Group II

Nonidentical MQWs of group I are composed of four QWs with different widths, similar to stacking four single QWs. The energy coupling may not be strong in this structure, so the second group of mirror-imaged nonidentical MQWs is designed, fabricated, and measured.

2.2.1 Nonidentical MQW Design and Fabrication

Layer structures of the second group are shown in Fig. 5. Two sets of MQWs, 6nm $In_{0.67}Ga_{0.33}As_{0.72}P_{0.28}$ triple QWs (designed approximately for lasing wavelength λ=1.3μm) and 8.7nm $In_{0.53}Ga_{0.47}As$ double QWs (designed approximately for λ=1.55μm), form the basic components of the nonidentical MQW structure. Substrate 04291 has the $In_{0.53}Ga_{0.47}As$ double QWs near the n-cladding layer while 04292 has this set near the p-cladding. The other set is arranged in sequence. The QWs are bounded by 15nm $In_{0.86}Ga_{0.14}As_{0.3}P_{0.7}$ barrier and the SCH region is 120nm with the same component as barrier. Detailed calculations of the emission spectra show that the transition energies of the 8.7nm $In_{0.53}Ga_{0.47}As$ double QWs are 1.54μm, 1.46μm, and 1.18μm. The transition energies of the 6nm $In_{0.67}Ga_{0.33}As_{0.72}P_{0.28}$ triple QWs are 1.30μm and 1.24μm.

04291 and 04292 are then grown lattice-matched to InP substrate. The grown nonidentical MQW structures are then used to fabricate ridge-waveguide LDs by the same procedures described before. The ridge waveguide was created by ECR- RIE.

Etching was stopped at ~100nm above the SCH layer. The devices are about 500μm long. The measured optical characteristics are shown and discussed in the next section.

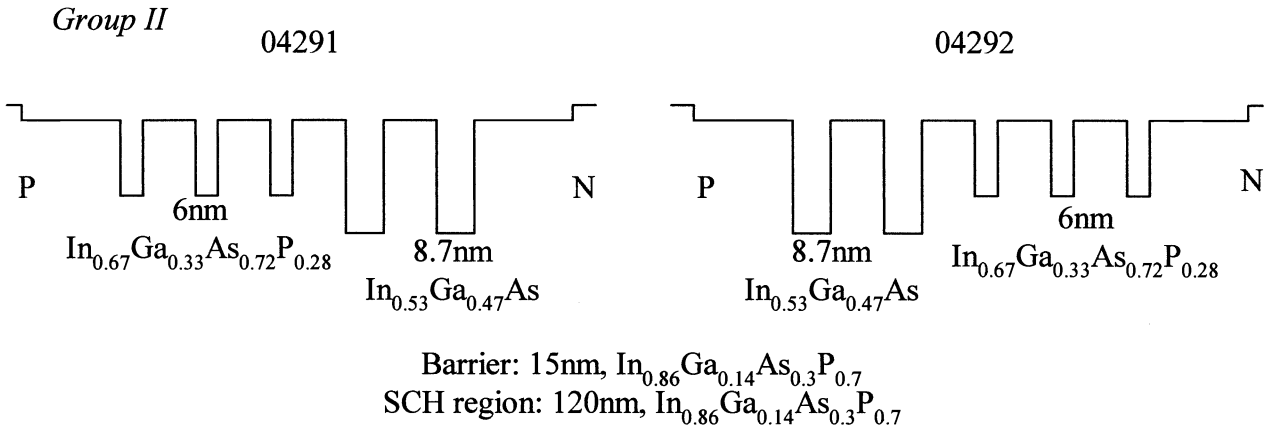

Fig. 5 Layer structures of Group II mirror-imaged nonidentical MQW, 04291 and 04292

2.2.2 Device Characteristics

L-I characteristics under temperature varying from 20℃ to 55℃ and the lasing spectra of the fabricated devices are then measured. The results are shown in Fig. 6 and Fig. 7. The sequence of QWs again has very important influences on the characteristics of the LDs. The threshold currents of both substrates are almost the same when temperature is below 30℃. However, when temperature is over 30℃, significant difference between 04291 and 04292 LDs is observed. 04291 LDs have larger I_{th} than 04292 under higher temperature. Curve fitting shows that characteristic temperature of 04292 is always much higher than that of 04291, indicating much more temperature sensitive behavior of 04291 than 04292 LDs. The differential quantum efficiency η_d of 04291 LDs is always lower than 04292 LDs, and decreases with increasing temperature. On the other hand, η_d of 04292 maintains approximately the same except for temperature around 30℃, rather than decrease with temperature. Further measurement shows that lasing wavelength changes around that temperature.

Lasing spectra of both LDs are shown in Fig. 7. Substrates 04291 and 04292 have the lasing wavelength at around 1500nm and around 1415nm, respectively. Referring to the layer structure in Fig. 5, the difference in lasing wavelength shows that QWs near the n-cladding contribute more to emission. This also indicates the electron-dominated carrier distribution. Furthermore, the lasing wavelengths of 04292 and 04291 LDs could randomly occur in a spectral range of about 20nm when the bias current is at the same level. The reason is due to the very flat plateau of gain profile, leading to the start-up noise significantly influencing the final lasing wavelength, like chaotic behaviors.

Stacking of different MQWs with the different width causes the more complicated behaviors, resulting in complexities for analyzing the carrier distribution. Although the lasing spectra of 04291 and 04292 imply that electron is still the dominant carrier for both substrates 04291 and 04292, this property cannot be distinguished easily from figures of I_{th} and η_d vs.

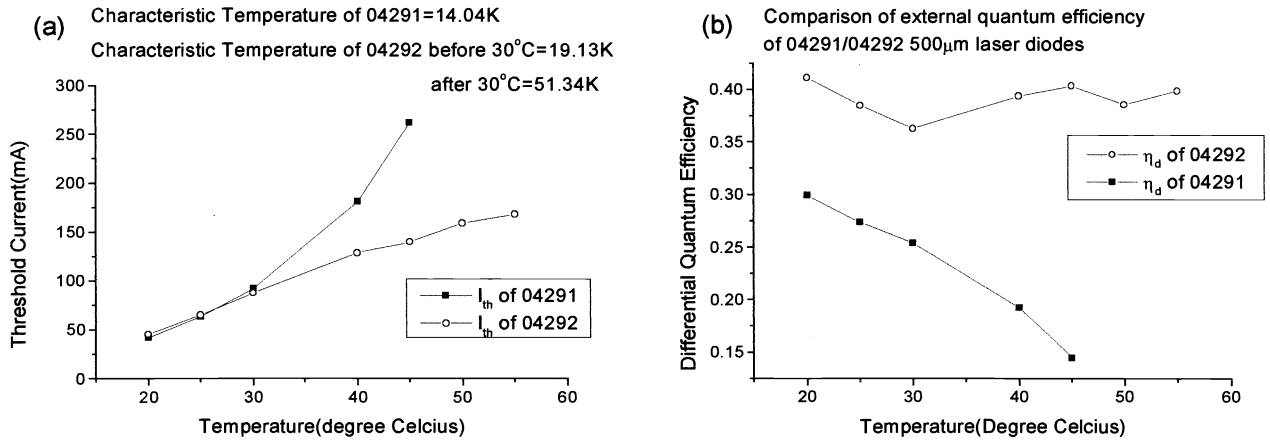

Fig. 6 (a) Threshold current and (b) differential quantum efficiency of 04291 and 04292 measured in different temperature.

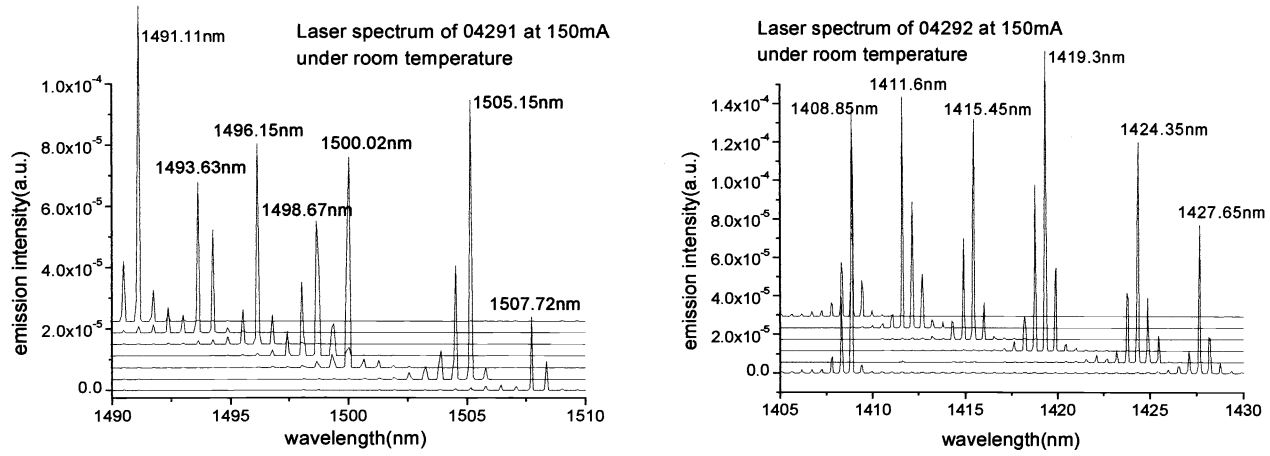

Fig. 7 Measured lasing spectra of 04291(Left) and 04292 (right) at fixed current of 150mA

temperature. This is resulted from anisotropic increment of gain between the two sets of MQWs with different well numbers. Peak gain versus carrier density in each well is calculated by extracting peak gain in gain spectra simulated using Luttinger-Kohn model.[8] The figure is shown in Fig. 8. For group I of nonidentical MQWs, which consist of stacking of single QW of different widths, the QW corresponding to longest emission wavelength always has the highest gain under the same carrier density in each well. Hence the lasing wavelength is always contributed from the widest QW and I_{th} and η_d vs. temperature relations can be easily interpreted. However, in group II, for single QW case, 1.55μm $In_{0.53}Ga_{0.47}As$ QW has higher gain than 1.3μm $In_{0.67}Ga_{0.33}As_{0.72}P_{0.28}$ QW at all times. The gain of 1.3μm $In_{0.67}Ga_{0.33}As_{0.72}P_{0.28}$ triple QWs surpasses that of 1.55μm $In_{0.53}Ga_{0.47}As$ double QWs over certain carrier density in each well. This causes the complexity and no straightforward explanation of I_{th} and η_d vs. temperature can be deduced. Internal loss needs to be measured to estimate the

carrier density in each well and thereby to ensure the gain relation between 1.3μm triple QWs and 1.55μm double QWs. For now, using evidences such as spectra of LDs and superluminescent diodes (SLDs)[9], electron being the dominant carrier is confirmed.

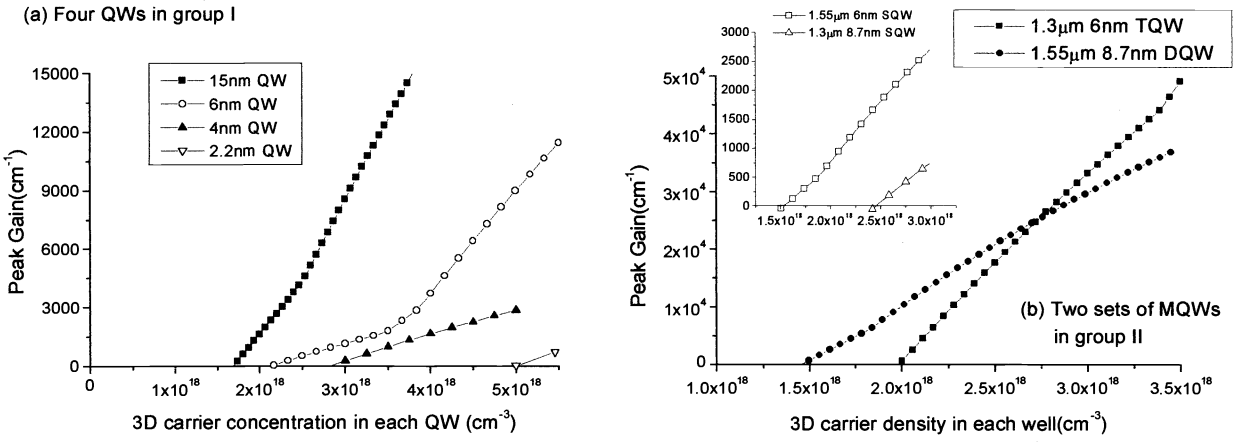

Fig. 8 Simulated peak gain vs. carrier density in each well of (a)four single QWs in Group I, and (b)MQWs in Group II

From Fig. 6(b), due to the extraordinary η_d vs. temperature behavior of 04292, lasing wavelengths under various temperatures are measured and shown in Fig. 9. 04292 LDs demonstrate novel wavelength switching that change from 1417nm below 30℃ to 1370nm over 35℃. A 47nm lasing wavelength switch is controlled by temperature variation of 5°C. The mechanism of this novel behavior is still under investigation and should be related to temperature dependant carrier transport and escape.

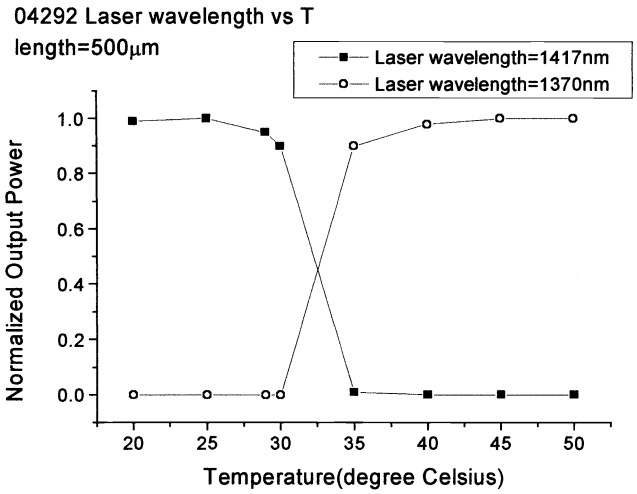

Fig. 9 Measured lasing wavelength vs. temperature of 04292 LDs

3. DISCUSSION

3.1 Carrier Transport Effects inside MQW

Carrier transport effects are briefly described in section 1. Contemporary model includes carrier transport in unconfined 3D regions, whose behavior can be governed by classical diffusion/drift model in ordinary semiconductor structures. When carriers transport near the QW region, sequential capture/escape of 3D carriers into 2D quantized QW states take place. These processes all cause time delays and hence degrade the dynamic properties of MQW devices. Carrier distribution, as a steady state of carrier transport, is related to the transport delay of the carrier dynamics. The delay times can be divided into two categories: delay time of carrier transport across the unconfined 3D SCH regions (classical diffusion and drift model is considered), and delay time of 3D carrier capture into 2D QW structures.[10] The total delay time then determines whether electrons or holes are transferred faster from 3D states into quantized 2D states, and moreover, determines the dominant carrier. Carrier capture rate is proportional to the density of states, meaning holes have a higher capture rate than electrons. Therefore the delay time of holes captured into QW is shorter than that of electrons. However, due to the higher mobility of electrons, they transport faster over the SCH region than holes. Thus the delay time of electrons transport across the SCH region is shorter than that of holes. As a result, whether electrons or holes have the shorter total delay time is left undetermined. Detailed estimation is required to understand which type of carriers dominates the carrier distribution. The relation of total delay times of electron and hole are listed below:

$$\tau_{total,\,n} = \tau_{n,diffusion} + \tau_{n,cap} = \frac{d_n^2}{4D_n} + \tau_{n,cap}$$
$$\tau_{total,p} = \tau_{p,diffusion} + \tau_{p,cap} = \frac{d_p^2}{4D_p} + \tau_{p,cap} \qquad (1)$$

Where d_n and d_p are the distance for electron and hole to diffuse across the QW structure, mainly the length of the SCH region; D_n and D_p are the diffusion coefficient of electron and hole, which depend on material component; and $\tau_{n,cap}$ and $\tau_{p,cap}$ are the quantum mechanical capture time for electron and hole, which are generally assumed to be 1ps and 0.2ps, respectively. The criterion to determine the dominant carrier using total time is as follows. If the total delay time of electron is shorter than that of hole, then electron is the dominant carrier; and vice versa for hole. The calculation result of (1) on the designed MQWs are shown in Table I.

Table I Calculated results of the total delay time of the nonidentical MQW structures

	$\tau_{n,diffusion}$	$\tau_{p,diffusion}$	$\tau_{n,cap}$	$\tau_{p,cap}$	$\tau_{n,total}$	$\tau_{p,total}$
Group I05111/05112	0.18ps	6.17ps	1ps	0.2ps	1.18ps	6.37ps
Group II04291/04292	0.34ps	11.52ps	1ps	0.2ps	1.34ps	11.72ps

From table I it is obvious that the long SCH region results in long hole diffusion time, which causes the electron-dominated carrier distribution. The diffusion coefficients for electron and hole depend on material components. Quantum mechanical carrier capture time should also depend on material parameters (such as material ingredients and strain) and QW structures (layer structure which alters the DOS), but the time scale seems negligible compared to classical carrier diffusion time. This implies that we can decide whether electron or hole is the dominant carrier by adjusting SCH region material and SCH region length. For narrow SCH region, hole has better chance being the dominant carrier, while electron should dominate carrier distribution for wide SCH region. The critical SCH region length below which hole is the dominant carrier and above which electron is the dominant carrier depends also on material parameters and QW structures.

4. CONCLUSION

Using mirror-imaged nonidentical MQW structures, we can clearly distinguish the distribution characteristic of MQW. In this work, lasers of nonidentical MQW structures are designed, fabricated, and measured. Electron-dominated distribution behavior is observed for the first time. The long SCH region, which takes holes more time to transport across, is the main reason for the observed behaviors. Electron- or hole-dominated carrier distribution can be designed by considering the MQW layer structure and material parameters. The above experiments show that LDs with nonidentical QWs involve more physics than those with conventional QWs of the same widths. Thus more functions might be achieved using nonidentical MQWs.

REFERENCES

1. Y. Arakawa and A. Yariv, "Quantum well lasers – gain, spectra, dynamics", *IEEE J. Quantum Electron.* Vol. 22, pp. 1887-1899, 1986.
2. R. M. Spencer, J. Greenberg, L. F. Eastman, C. Y. Tsai, and S. S. O'keefe, "High speed direct modulation of semiconductor lasers," from *High Speed Diode Lasers*, Editor: S. A. Gurevich, pp. 41-80, World Scientific, Singapore, 1998.
3. N. Tessler and G. Eisenstein, "Distributed nature of quantum well lasers," *Appl. Phys. Lett.*, vol. 63, pp. 10-12, 1993.
4. N. Tessler and G. Eisenstein, "On carrier injection and gain dynamics in quantum well lasers", *IEEE J. Quantum Electron.*, vol. 29, pp.1586-1595, 1993.
5. B. L. Lee, C. F. Lin, J. W. Lai, and W. Lin, "Experimental evidence of nonuniform carrier distribution in multiple-quantum-well laser diodes," *Electron. Lett.*, vol. 34, pp. 1230-1231, 1998.
6. H. Yamazaki, A. Tomita, and M. Yamaguchi, "Evidence of nonuniform carrier distribution in multiple quantum well lasers", *Appl. Phys. Lett.*, vol. 71, pp. 767-769, 1997.
7. D. Tauber and J. E. Bowers, "Dynamics of wide bandwidth semiconductor lasers," from *High Speed Diode Lasers*, Editor: S. A. Gurevich, pp. 1-40, World Scientific, Singapore, 1998.
8. Ahn, D. and Chuang, S. L.: "Optical gain and gain suppression of quantum well lasers with valence band mixing",

IEEE J. of Quantum Electron., vol. 26, pp. 13-24, 1990.

9. C. F. Lin, B. R. Wu, L. W. Laih, and T. T. Shih, "Sequence Influence of Nonidentical InGaAsP Quantum Wells on Broadband Emission", *IEEE Photon. Technol. Lett.* (in revision)
10. M. Alam and M. Lundstrom, "Simple analysis of carrier transport and buildup in separate confinement heterostructure quantum well lasers", *IEEE Photon. Technol. Lett.*, vol. 6, pp. 1418-1420, 1994.